Clinical Chemistry 47:6
1068–1074 (2001)

Endocrinology and Metabolism

Nitric Oxide Measurements during Endotoxemia

Viktor Brovkovych,[1] Lawrence W. Dobrucki,[1] Svitlana Brovkovych,[1]
Iwona Dobrucki,[1] Leszek Kalinowski,[*] Frederick Kiechle,[2] and Tadeusz Malinski[1†]

Background: **Excessive continuous NO release from inducible NO synthase over prolonged periods under pathological conditions, such as endotoxemia, contributes significantly to circulatory failure, hypotension, and septic shock. This NO production during endotoxemia is accompanied by superoxide release, which contributes to the fast decay of NO. Therefore, the amount of NO that diffuses to target sites may be much lower than the total amount released under pathological conditions.**

Methods: **We performed in vivo and ex vivo measurements of NO (electrochemical) and ex vivo in situ measurements of superoxide, peroxynitrite (chemiluminescence), and nitrite and nitrate (ultraviolet-visible spectroscopy). We determined the effect of lipopolysaccharide administration (20 mg/kg) on diffusible NO, total NO (diffusible plus consumed in chemical reactions), and superoxide and peroxynitrite release in the pulmonary arteries of rats.**

Results: **An increase in diffusible NO generated by constitutive NO synthase was observed immediately after administration of lipopolysaccharide, reaching a plateau (145 ± 18 nmol/L) after 540 ± 25 s. The plateau was followed by a decrease in NO concentration and its subsequent gradual increase after 45 min because of NO production by inducible NO synthase. The concentration of superoxide increased from 16 ± 2 nmol/L to 30 ± 3 nmol/L after 1 h and reached a plateau of 41 ± 4 nmol/L after 6 h. In contrast to the periodic changes in the concentration of diffusible NO, the total concentration of NO measured as a sum of nitrite and nitrate increased steadily during the entire period of endotoxemia, from 2.8 ± 0.2 μmol/L to 10 ± 1.8 μmol/L.**

Conclusions: **The direct measurement of NO concentrations in the rat pulmonary artery demonstrates dynamic changes throughout endotoxemia, which are related to the production of superoxide and the subsequent increase in peroxynitrite. Monitoring endotoxemia with total nitrate plus nitrite is not sensitive to these fluctuations in NO concentration.**

Endotoxemia is defined as an alteration in cellular oxygen metabolism initiated by infection. Excessive production of NO has been implicated in the pathogenesis of endotoxemia *(1)*. Inducible NO synthase (iNOS)[3] activity stimulated at the site of infection is primarily responsible for the sustained release of NO *(2)*. The increase in NO leads to myocardial depression *(3)* and vascular dysfunction associated with vasorelaxation and hypotension. Decreased skin perfusion, reduced mental alertness, and increased serum lactate concentrations are also characteristics of endotoxemia *(4)*. Endotoxemia remains the main cause of death in intensive care units. It has a mortality rate in the US of 50–60% *(5)*. The release of multiple endogenous mediators plays a causative role in initiating an uncontrolled inflammatory response *(6)*. One of those mediators has been identified as NO.

NO is generated by two constitutive NOS (cNOS) isoforms, endothelial NOS (eNOS) and neuronal NOS (nNOS), which control relaxation of smooth muscles and modify central and peripheral nervous system function. Dysfunction of cNOS is associated with reduced production of NO, which leads to severe ischemia/reperfusion injury, hypertension, and hypercholesterolemia *(7)*. In contrast, excessive and continuous production of NO by iNOS over prolonged periods contributes significantly to

[1] Department of Chemistry and Biochemistry, Ohio University, Athens, OH 45701.

[2] Department of Clinical Pathology, William Beaumont Hospital, Royal Oak, MI 48073.

*On sabbatical leave from: Department of Biochemistry, Medical University of Gdansk, and Laboratory of Cellular and Molecular Nephrology, Medical Research Center of the Polish Academy of Science, 80-210 Gdansk, Poland.

†Address correspondence to this author at: Department of Chemistry and Biochemistry, Ohio University, Clippinger Laboratories, Athens, OH 45701. Fax 740-593-9641; e-mail malinski@ohio.edu.

Received January 19, 2001; accepted March 15, 2001.

[3] Nonstandard abbreviations: i-, c-, e-, and nNOS, constitutive, inducible, endothelial, and neuronal NO synthase; LPS, lipopolysaccharide; L-NMMA, N^G-monomethyl-L-arginine; L-NIL, L-N^6-(1-iminoethyl)-lysine; HBSS, Hank's balanced salt solution; and PEG-SOD, polyethylene glycol–superoxide dismutase.

circulatory failure and hypotension as observed during endotoxemia *(8)*. Several endotoxins activate the transcription and translation of iNOS, the third NOS isoform *(9)*. This induction of iNOS occurs mainly in leukocytes, macrophages, hepatocytes, cardiac myocytes, and, to a lesser degree, in vascular smooth muscle *(8)*. Induction of iNOS at the site of infection is responsible for the massive and uncontrolled generation of NO, which occurs during endotoxemia *(2, 6)*.

Cytotoxicity is often directly attributed to NO. However, NO is only moderately reactive and shows low cytotoxicity at physiologic concentrations *(10)*. The major decay route for NO in mammalian systems is by its extremely rapid reaction with superoxide (O_2^-) to form peroxynitrite ($OONO^-$; Fig. 1). It is one of the fastest reactions in mammalian physiology ($K = 6.7 \times 10^9$ $L \cdot mol^{-1} \cdot s^{-1}$) *(11)*. The final product (peroxynitrite) is usually harmless. However, after protonation ($pK_a = 6.8$), peroxynitric acid is formed, which, at high concentrations, is very cytotoxic. Peroxynitric acid undergoes either homolytic cleavage to form the hydroxyl free radical ($OH^{\cdot}$) and the nitrogen dioxide free radical ($NO_2^{\cdot}$) or heterolytic cleavage to form the nitronium cation (NO_2^+) and the hydroxide anion (OH^-) *(12)*. These three extremely reactive moieties ($OH^{\cdot}$, $NO_2^{\cdot}$, and NO_2^+) are most likely the source of the observed cytotoxicity erroneously attributed to NO *(13)*.

The total concentration of NO during endotoxemia has been estimated by the determination of the concentration of NO decay products ($NO_2^- + NO_3^-$). This indirect approach has demonstrated a significant increase in the concentration of $NO_2^- + NO_3^-$ during endotoxemia as measured in a variety of body fluids *(9, 14, 15)*. However, these measurements provide no information concerning diffusible active NO, which is capable of activating smooth muscle relaxation. The diffusible NO plays a crucial role in hypotension during endotoxemia. Therefore, the indirect measurement of NO degradation products ($NO_2^- + NO_3^-$) may provide very misleading information concerning the degree of vasorelaxation within the cardiovascular system.

This report describes both direct electrochemical measurements of the diffusible concentration of NO (active NO concentration) and indirect measurements of the NO final decay products (total amount of NO produced is expressed as a sum of NO_2^- and NO_3^- concentration) during endotoxemia in an animal model. These results were correlated with chemiluminescence measurements of O_2^- and peroxynitrite, which are generated simultaneously with NO during endotoxemia.

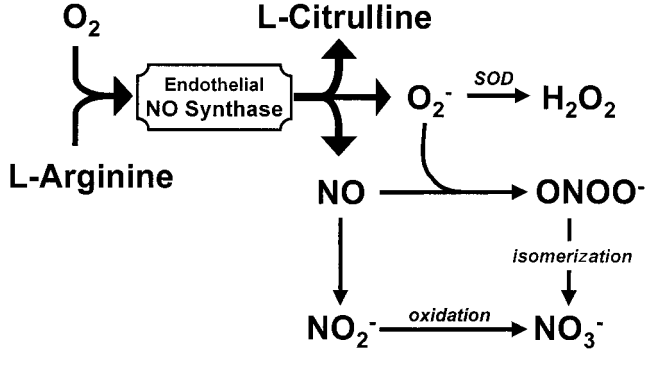

Fig. 1. Schematic diagram showing the L-arginine pathway in the dysfunctional endothelium under pathological conditions.

Materials and Methods

ANIMALS

Normotensive Wistar-Kyoto male rats (280–320 g) were maintained at 22 ± 1 °C with a 12-h light/12-h dark cycle and were allowed water and standard rat chow ad libitum.

SURGERY

Rats were anesthetized with an intraperitoneal injection of a mixture of 100 mg/kg ketamine and 10 mg/kg xylazine. They were intubated and ventilated with room air using a Harvard small animal ventilator set at a tidal volume of 2.5 mL and a breathing rate of 100 breaths/min. The porphyrinic NO sensor was placed in a pulmonary artery wall during the surgery, and its exact localization was determined during postmortem examination. Polyurethane catheters were inserted into the left jugular and left femoral veins for drug administration. The endotoxin lipopolysaccharide [(LPS); *Escherichia coli* serotype 0127: B8; Sigma] was dissolved in saline and subsequently administered as an intravenous infusion ($2\ mg \cdot kg^{-1} \cdot min^{-1}$ for 10 min; total dose, 20 mg/kg). N^G-Monomethyl-L-arginine (L-NMMA), a nonspecific cNOS and iNOS inhibitor, was purchased from Sigma Chemical, and L-N^6-(1-iminoethyl)-lysine (L-NIL), a selective iNOS inhibitor, was from LC Laboratories Co. Each of the inhibitors was dissolved in 0.1 mol/L phosphate buffer (pH 7.4) and then injected as an intravenous bolus (20 mg/kg) 45 min before the start of the LPS infusion. Another catheter was placed in the right carotid artery for intermittent blood sampling.

PREPARATION OF PULMONARY ARTERY FOR IN VITRO MEASUREMENTS

The isolated pulmonary artery was placed in modified Hank's balanced salt solution (HBSS; Sigma) at 4 °C and pH 7.4. The composition of HBSS is as follows: NaCl (137 mmol/L), Tris-HCl (10 mmol/L), $MgCl_2$ (1 mmol/L), KCl (5 mmol/L), $CaCl_2$ (1.8 mmol/L), $MgSO_4$ (0.8 mmol/L), KH_2PO_4 (0.44 mmol/L), Na_2HPO_4 (0.33 mmol/L), and L-arginine (0.1 mmol/L). Under the dissection microscope (Wild M3G; Leica), the pulmonary artery was cleared of adjacent tissue and cut into small segments (2–3 mm). When polyethylene glycol–superoxide dismutase (PEG-SOD; Sigma) was used, it was added to HBSS at a dose of 100 kU/L of medium 10 min before injection of the calcium ionophore (A23187).

preparation of NO sensors for in vitro and in vivo measurements

Two types of NO sensors were used for the in vivo and in vitro experiments. Their design was based on previously developed and well-characterized, chemically modified carbon-fiber technology *(16–18)*. The porphyrinic sensor is free of interference from all reagents used in these experiments and from substances that may have been found in mammalian blood to concentrations at least two orders of magnitude greater than their expected concentrations. The NO sensor is also insensitive to blood pressure changes *(19)* and has a small thermal coefficient (1.8% of signal/°C). Additionally, the sensor is free of piezoelectric noise and is not affected by induced currents generated by contracting muscles of the cardiac systems *(16, 20)*. The catheter-protected porphyrinic NO sensor for in vivo measurements was mounted on the tip of a truncated needle. Briefly, the needle from an intravenous catheter unit, 24 gauge and 25 mm long (Angiocath; Becton Dickinson), was roughened along the shaft and then truncated and polished flat, so that it was 3 mm shorter than its 24-gauge, protective catheter. A bare copper wire with a diameter of 0.1 mm and coated with conducting epoxy and a single carbon fiber (6 μm in diameter; protruding 3 mm) were mounted inside the hollow needle on the protruding carbon-fiber tip. A highly conductive polymeric porphyrin was deposited on the protruding carbon-fiber tip by the use of 0.50 mmol/L nickel(II) tetrakis(3-methoxy-4-hydroxyphenyl)porphyrin (TMHPPNi) in 0.1 mol/L NaOH and the cyclic voltammetry deposition technique. After the deposition process, the carbon fiber tip was immersed three times for 6–7 s in a 10 g/L alcohol solution of Nafion (Aldrich).

For in vivo measurements, smooth muscle tissue was pierced with the catheter needle and positioned at the desired place in the pulmonary arterial wall. When the position of the catheter was secure, the needle was removed and replaced with the porphyrinic sensor. The auxiliary electrodes, platinum and silver/silver chloride (SSCE) electrodes, were placed in contact with the adjacent tissue. For in vitro measurements, an open arterial strip was placed in a thermostated organ chamber and two auxiliary electrodes of the three-electrode system (the platinum as a counter electrode and the silver/silver chloride as a reference electrode) were positioned in the organ chamber near the arterial strip. The porphyrinic sensor without catheter protection was lowered near the surface (5 $\pm$ 2 μm) of the previously positioned opened arterial ring with the aid of the dissecting microscope and micromanipulator. Chronoamperometry was used for fast (0.1-s response time) and continuous measurement of the change of NO concentration with time. The data were collected using a PAR model 273 voltammetric analyzer (EG&G Princeton Applied Research) interfaced with an IBM Pentium computer with data acquisition and control software (Research Electrochemistry Software, Ver. 4.30; EG&G Princeton Applied Research). Before and after in vivo and in vitro measurements, each sensor was calibrated using NO calibration solutions at NO concentrations of 2×10^{-9} to 2×10^{-5} mol/L prepared as described previously *(21)*.

NO_2^- and NO_3^- measurements

At the same time as the electrochemical measurements of active NO in the tissue during endotoxemia, indirect measurements of NO_2^- and NO_3^- (final products of NO decay) were performed using the Griess method *(22)*. The Griess reagent is specific for NO_2^-; therefore, NO_3^- was reduced to NO_2^- by metallic cadmium. NO_2^- and NO_3^- content was determined as NO_2^- from absorbance measurements at 540 nm using a calibration curve.

superoxide measurements

The concentration of O_2^- was determined by a chemiluminescence method *(23)*. O_2^- produced chemiluminescence from lucigenin (bis-*N*-methylaridinium NO_3^-; Sigma), which was detected by a scintillation counter (Beckmann 6000 LS with a single-photon monitor). Each tissue sample (0.8–1.5 mg) was immersed in 2 mL of HBSS adjusted to pH 7.4 at 25 °C. Lucigenin was added to the solution to a final concentration of 0.25 mmol/L. All measurements of O_2^- were made in a similar manner after a 2-min incubation in HBSS. For the nonbasal determination of O_2^-, the 2-min incubation period was followed by the injection of 20 μL of 1 mmol/L A23187 calcium ionophore. A23187 is a receptor-independent cNOS agonist and is needed to measure maximal cNOS production of NO. Calibration curves were constructed on the basis of the photons emitted by the O_2^- generated after treatment of xanthine with xanthine oxidase.

peroxynitrite measurements

A chemiluminescence method was also used to determine the concentration of peroxynitrite *(22)*. Photon counts were recorded with a scintillation counter (Beckman 6000LS, with a single-photon monitor). Each tissue sample (8–10 mg) was immersed in 0.5 mL of HBSS adjusted to pH 7.4 at 25 °C, and then calcium ionophore A23187 solution was added to a final concentration of 20 μmol/L. Alkaline sodium bicarbonate luminol solution (1.0 mL) was added after 3 s to achieve a final concentration of 400 μmol/L luminol (5-amino-2,3-dihydro-1,4-phthalazinedione) and 50 mmol/L bicarbonate at pH 10.0. The basal concentration of peroxynitrite was obtained in the same manner in the absence of tissue.

statistical analysis

Values were expressed as means $\pm$ SE, with $P < 0.05$ considered statistically significant. Statistical evaluation was done by ANOVA followed by unpaired Student *t*-test. All analyses were performed with the statistical software Microcal Origin (Microcal Software, Inc.).

Results

NO PRODUCTION

The total concentration of NO_2^- and NO_3^- in blood plasma increases during endotoxemia induced by administration of LPS (Fig. 2). After 3 h of endotoxemia, a statistically significant increase in the total concentration of NO_2^- plus NO_3^- was observed, which reached a plateau of 10 ± 1.8 μmol/L after 5 h. The plateau concentration was approximately fourfold higher than the basal concentration.

However, the direct, in vivo electrochemical measurement of NO using the porphyrinic sensor implanted into the rat pulmonary artery clearly showed two phases of NO release during endotoxemia (Fig. 3a). In the early acute phase, after administration of 20 mg/kg LPS, a sharp increase in the production of NO above its basal concentration of 52 ± 10 nmol/L was observed. The rate of increase for NO was 0.19 $nmol \cdot L^{-1} \cdot s^{-1}$. After 540 ± 25 s, the NO concentration reached a plateau of 145 ± 18 nmol/L above the basal concentration that persisted for 4 ± 0.6 min. The plateau was followed by a decrease in the concentration of NO at the rate of -0.07 $nmol \cdot L^{-1} \cdot s^{-1}$. After 45 min, a second increase in the concentration of NO was observed, but at a much slower rate of <0.02 $nmol \cdot L^{-1} \cdot s^{-1}$. A second plateau of NO concentration was established 90 ± 10 min after administration of LPS. The selective inhibitor of iNOS, L-NIL, at the dose of 20 mg/kg decreased the NO concentration only during the second phase of endotoxemia (~5 min after LPS administration; Fig. 3B). Administration of the L-NMMA (20 mg/kg) nonselective inhibitor of eNOS, nNOS, and iNOS decreased the concentration of NO during both the acute phase and the second phase of endotoxemia (Fig. 3C).

To estimate the potential maximum concentration of NO produced by eNOS during endotoxemia, in vitro changes in endothelial NO concentration were measured in freshly excised pulmonary artery after stimulation with 10 μmol/L calcium ionophore A23187 (Fig. 4). The single carbon-fiber porphyrinic sensor was placed close (5 ± 2 μm) to the surface of the endothelial cells in an excised segment of pulmonary artery, and NO concentrations were recorded at different times after the administration of LPS. To estimate the influence of O_2^- on calcium-stimulated endothelial NO release, NO was measured after endotoxemia in the presence or absence of 100 kU/L PEG-SOD (membrane-permeable SOD). The basal con-

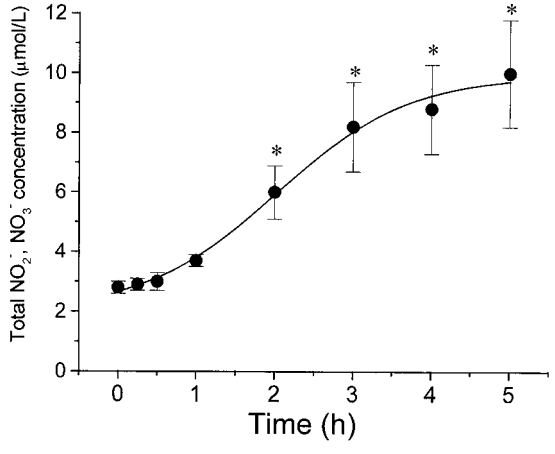

Fig. 2. Changes of total NO_2^- and NO_3^- concentration in blood plasma during endotoxemia induced by administration of LPS (20 mg/kg; n = 6).
*, $P < 0.01$ vs control (without LPS).

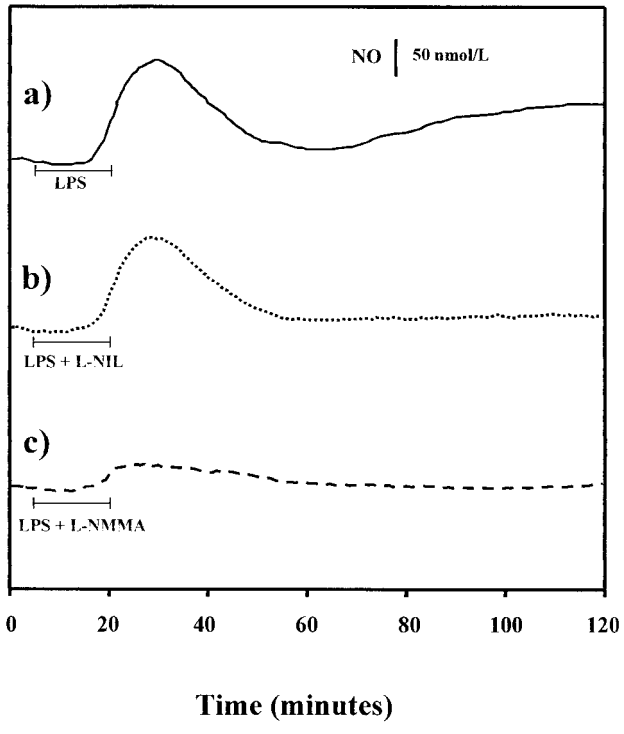

Fig. 3. In vivo measurement of NO release in rat pulmonary artery during the first 120 min after administration of LPS (20 mg/kg; *a*) and after administration of LPS and the same dose (20 mg/kg) of iNOS inhibitors L-NIL (*b*) and L-NMMA (*c*).

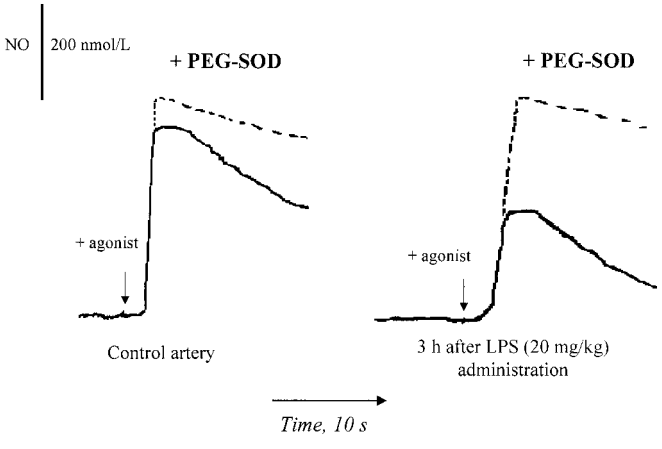

Fig. 4. Typical in vitro amperograms showing NO release from pulmonary artery of a rat before (*left*) and 3 h after (*right*) administration of LPS (20 mg/kg).
The NO release was stimulated with calcium ionophore (A23187; 10 μmol/L) in the absence (*solid line*) and presence (*dashed line*) of PEG-SOD (100 kU/L).

centration of NO was 45 ± 5 and 27 ± 8 nmol/L in control and endotoxic tissue, respectively. In the presence of PEG-SOD, the basal concentration significantly increased in endotoxic (40 ± 3 nmol/L), but not in the control (48 ± 5 nmol/L). NO release stimulated by calcium ionophore in the controls was increased by 15% from 437 ± 6 nmol/L to 504 ± 7 nmol/L in the presence of PEG-SOD. However, in endotoxic artery, the concentration of NO increased by ~50% in the presence of PEG-SOD (increase from 262 ± 3 nmol/L to 547 ± 5 nmol/L; $P < 0.001$; n = 6).

Endothelial NO production was substantially decreased during the first 3 h of endotoxemia (Figs. 4 and 5) because of the increased generation of O_2^-. The increase of O_2^- was confirmed indirectly with an experiment performed in the presence of PEG-SOD. In the presence of PEG-SOD, the NO concentration was restored to the concentration observed before endotoxemia. The maximal production of NO by endothelium during different phases of endotoxemia was determined by activating cNOS with the receptor-independent agent A23187 (Fig. 5; n = 6).

SUPEROXIDE GENERATION

The previous experiments using PEG-SOD suggest that the increase in the production of O_2^- during endotoxemia is responsible for the decrease in the concentration of NO (Figs. 4 and 5). During the time period (60 min) of endotoxemia, there was no significant decrease in the eNOS protein as determined by Western blot. Therefore, the decrease of the production of NO is attributable solely to an increase in the generation of O_2^-. To confirm this hypothesis, a chemiluminescence method was used to directly measure the concentration of O_2^- during endotoxemia in freshly isolated tissue. The mean basal concentration (before endotoxemia) of O_2^- in the pulmonary artery was 16 ± 2 nmol/L (Fig. 6). The change in the total concentration of O_2^- with time after LPS administration was measured after the maximal stimulation of NO release by A23187 (Fig. 6). One hour after LPS administration, the concentration of O_2^- increased to 30 ± 3 nmol/L, reaching a plateau of 41 ± 4 nmol/L after 6 h (Fig. 6; n = 6). In the presence of L-NMMA, the concentration of O_2^- decreased ~60%. The decrease in O_2^- concentration is similar to the decrease in the NO concentration in the presence of L-NMMA.

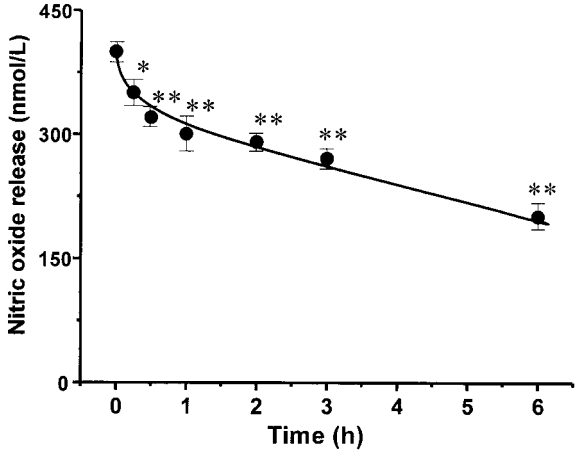

Fig. 5. NO release from the pulmonary artery plotted vs the time of endotoxemia.

The NO release was stimulated with calcium ionophore (A23187; 10 μmol/L) in excised segments of pulmonary artery at different times after the administration of LPS (20 mg/kg; n = 6). *, $P < 0.05$; **, $P < 0.01$ vs control (without LPS).

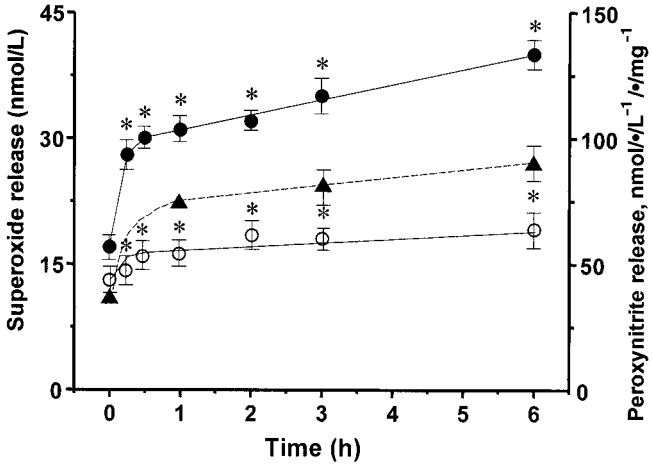

Fig. 6. In vitro chemiluminescence measurements of total superoxide concentration (*solid line*) and ultraviolet spectroscopic measurements of peroxynitrite (*dashed line*) in the tissue of pulmonary artery during endotoxemia.

Superoxide (●, ○) and peroxynitrite (▲) were measured after the maximal stimulation of NO release with calcium ionophore (A23187; 10 μmol/L) after incubation with LPS (20 mg/kg; n = 6). Superoxide was measured without (●) and with the addition of L-NMMA (○). *, $P < 0.01$ vs control (without LPS).

PEROXYNITRITE PRODUCTION

Peroxynitrite release was measured in vitro during the maximal stimulation of the release of NO by A23187 (Fig. 7), and it paralleled the release of O_2^- (Fig. 6) throughout endotoxemia. After 1 h, the concentration of peroxynitrite

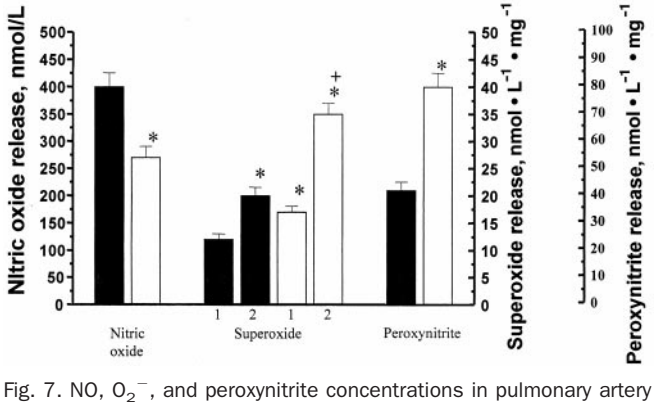

Fig. 7. NO, O_2^-, and peroxynitrite concentrations in pulmonary artery measured before LPS administration (■) and after 3 h of LPS (20 mg/kg) administration (□).

O_2^- release was measured after the maximal stimulation of NO with the calcium ionophore A23187 (10 μmol/L; n = 6; *, $P < 0.01$ vs without LPS; +, $P < 0.01$ vs basal O_2^- concentration).

increased approximately twofold compared with the control. A plateau was established after 3 h of endotoxemia. The maximum concentrations of NO, O_2^-, and peroxynitrite before and 3 h after LPS administration are shown in Fig. 7.

Discussion

The direct and continuous in vivo measurement of diffusible NO in the pulmonary artery during endotoxemia demonstrated two distinct increases in the concentration of NO with time (Fig. 3A). The first increase in the concentration of NO occurred ~10 min after the administration of LPS and was attributable to the activation of eNOS. A similar pattern of NO release is observed after stimulation of endothelial cells with typical agonists of NO, such as bradykinin or acetylcholine. The second increase in the diffusible concentration of NO was observed ~1 h after the onset of endotoxemia and was a result of the activation of iNOS. These direct electrochemical measurements of NO differ markedly from the indirect estimation of total NO by spectroscopic measurements of NO_2^- and NO_3^- concentrations. This indirect measurement of degradation products revealed a steady increase in the concentration of NO with time during endotoxemia (Fig. 2). Therefore, the distinct biphasic temporal fluctuations detected in the concentration of biologically active NO by the porphyrinic microsensor were not detected with the less sensitive and more indirect method of measuring NO degradation products. The in vivo measurement of NO may be performed with the use of a modified porphyrinic microsensor placed in a catheter or needle, which can be located in tissue or in circulating blood for the direct determination of NO *(17)*. Although technically more demanding, this method provides a precise measurement of fluctuations of NO concentrations with time.

The measurement of NO and its metabolites in septic patients poses a challenge to the clinical laboratory. The indirect spectroscopic measurement of NO_2^- and NO_3^-, indicators of NOS activity and the total production of NO, is based on the detection of the degradation products of NO in plasma or urine *(13, 22)*. However, experimental evidence supporting the validity of this assumption is limited. In a recent study, mice lacking the *eNOS* gene had 40% less plasma NO_2^- and NO_3^- compared with wild-type mice *(24)*. Thus, the absence of eNOS leads to a reduction in plasma NO_2^- and NO_3^- not compensated by other NOS isoforms. However, this measurement still fails to account for temporal variations in concentrations of NO in plasma and specific organs *(2)*.

The evaluation of NO_2^- and NO_3^- in urine also has important limitations. The rate of excretion of NO_2^- and NO_3^- in the urine is directly related to renal function *(25)*. NO is generated from the following reaction: L-arginine + NADPH + O_2 → N^G-hydroxyl-L-arginine → citrulline + NO + $NADP^+$ *(26)*. The cellular elements in infected urine contain an increased amount of NO generated by iNOS compared with uninfected control specimens. The iNOS represents an endogenous source of NO_2^- production in the urine specimen *(27, 28)*. Under appropriate physiological conditions, NO and, therefore, its degradation products, NO_2^- and NO_3^-, can be produced nonenzymatically *(29–31)*. Hydrogen peroxide generates NO from D- or L-arginine by a nonenzymatic pathway *(30)*. The O_2^- anion oxidizes the intermediate, N^G-hydroxy-L-arginine, to NO *(30, 31)*. Therefore, inhibition of cNOS and/or iNOS activity, increased in septic shock *(32)*, will not completely stop NO production because the nonenzymatic synthetic pathways would not be altered. In acidic urine, some NO_2^- is converted to NO *(33)*. A variety of disease states lead to increased or decreased total production of NO and, therefore, alterations in NO_2^- excretion in the urine *(22, 34–36)*. Consequently, the concentration of NO_2^- and NO_3^- in urine is not only an indicator of a urinary tract infection, but also a monitor of the total body production of NO *(13, 22, 33–36)*.

The first phase of NO release during endotoxemia is catalyzed by calcium-dependent eNOS, which is activated by an increase in unbound cytosolic free calcium. Inhibition of calcium flux into the cell inhibits NO release *(1, 7)*. LPS activates intracellular calcium gradients, which stimulate eNOS to produce NO, water, and L-citrulline from L-arginine and O_2 *(8)* (Fig. 1). To estimate maximal cNOS activity at different times after the induction of endotoxemia, we used the calcium ionophore A23187 to increase intracellular calcium influx (Figs. 4–7). Concurrently, during this first phase of NO release, the concentration of O_2^- also increased (Fig. 6). This LPS-stimulated production of O_2^- is inhibited by the presence of the nonspecific NOS inhibitor L-NMMA. The generation of O_2^- occurs during endotoxemia after there is a local depletion of L-arginine of $<10^{-4}$ to 10^{-3} mol/L. At this low concentration of L-arginine, there is an insufficient concentration gradient for this substrate to bind to the active site of cNOS *(37)*. In the absence of L-arginine or tetrahydrobiopterin, cNOS function expands to the catalysis of two reactions: the one-electron reduction of O_2 to O_2^- and the five-electron oxidation of L-arginine to NO. When these two reactions take place in close proximity, the extremely rapid reaction of O_2^- with NO produces peroxynitrite, which, after protonation, rearranges to form the stable product NO_3^- *(9)*. Using isolated enzymes, Klatt et al. *(38)* found that both eNOS and nNOS, but not iNOS, can produce O_2^- in L-arginine- or tetrahydrobiopterin-limiting environments. Therefore, the decrease in the production of NO observed throughout endotoxemia (Fig. 5) can be attributed to the increased production of O_2^-. eNOS appears to be a major source of O_2^-. However, in endothelial cells, there are several other sources of O_2^- generation, including prostaglandin metabolism, cytochrome P450, and processes stimulated by protein kinase C or xanthine oxidase. Therefore, the net concentration of NO measured by the porphyrinic sensor depends not only on NO generated by cNOS, but also on the concentration of O_2^-. The increas-

ing concentration of O_2^- reacts with NO to produce peroxynitrite, which leads to a reduction in bioactive NO (Fig. 5), not a steady increase in NO as suggested by the determination of NO_2^- and NO_3^- (Fig. 2).

In conclusion, the indirect measurements of NO using the concentration of NO_2^- and NO_3^- during endotoxemia fails to provide an accurate release of bioactive NO. Because of the fast consumption of NO by O_2^-, the actual concentration of active NO in the cardiovascular system is relatively low, and this concentration can be monitored only by using direct, real-time measurement.

This work was supported by a grant from the William Beaumont Hospital Research Institute and Public Health Grant (HL 60900). We thank T. Kosaski for technical assistance in the preparation of the manuscript.

References

1. Titheradge MA. Nitric oxide in septic shock. Biochim Biophys Acta 1999;1411:437–55.
2. Annane D, Sanquez S, Sebille V, Fage Q, Djuzanovic D, Raphael JC, et al. Compartmentalised inducible nitric-oxide synthase activity in septic shock. Lancet 2000;355:1143–8.
3. Ronson RS, Nakamura M, Vinten-Johansen J. The cardiovascular effects and implications of peroxynitrite. Cardiovasc Res 1999; 44:47–59.
4. Vincent JL. Cardiovascular alterations in septic shock. J Antimicrob Chemother 1998;41(Suppl A):9–15.
5. Parrillo JE, Parker MM, Natanson C, Suffredini AF, Danner RL, Cunnion RE, et al. Septic shock in humans. Advances in the understanding of pathogenesis, cardiovascular dysfunction, and therapy. Ann Intern Med 1990;113:227–42.
6. Parratt JR. Nitric oxide. A key mediator in sepsis and endotoxaemia? J Physiol Pharmacol 1997;48:4,493–506.
7. Parratt JR. Nitric Oxide and cardiovascular dysfunction in sepsis and endotoxemia: an introduction and an overview. In: Schlag G, Redl H, eds. Shock, sepsis and organ failure—nitric oxide. Berlin: Springer Verlag, 1995:1–29.
8. Knowles RG, Moncada S. Nitric oxide synthase in mammals. Biochem J 1994;298:249–58.
9. Burgner D, Rockett K, Kwiatkowski D. Nitric oxide and infectious diseases. Arch Dis Child 1999;81:185–8.
10. Huie RE, Padmaja S. The reaction rate of nitric oxide with superoxide. Free Radical Res Commun 1993;18:195–9.
11. Beckman JS, Chen J, Ischiropoulos H, Crow JP. Oxidative chemistry of peroxynitrite. Methods Enzymol 1994;233:229–40.
12. Beckman JS, Koppenol WH. Nitric oxide, superoxide, and peroxynitrite: the good, the bad, and the ugly. Am J Physiol 1996;271: C1424–37.
13. Kiechle FI, Malinski T. Indirect detection of nitric oxide effects: a review. Ann Clin Lab Sci 1996;26:501–11.
14. Ahren C, Jungersten L, Sandberg T. Plasma nitrate as an index of nitric oxide formation in patients with acute infectious diseases. Scand J Infect Dis 1999;31:405–7.
15. Malinski T, Czuchajowski L. Nitric oxide measurements by electrochemical methods. In: Feelisch M, Stamler JS, eds. Methods in nitric oxide research. Chichester, UK: John Wiley & Sons, 1996: 319–39.
16. Malinski T, Taha Z. Nitric oxide release from a single cell measured in situ by a porphyrinic-based microsensor. Nature 1992;358:676–8.
17. Vallance P, Patton S, Bhagat K, MacAlliater R, Radomski M, Moncada S, et al. Direct measurement of nitric oxide in human beings. Lancet 1995;346:153–4.
18. Kubaszewski E, Peters A, McClain S, Bohr D, Malinski T. Light-activated release of nitric oxide from vascular smooth muscle of normotensive and hypertensive rats. Biochem Biophys Res Commun 1994;200:213–8.
19. Pinsky DJ, Patton S, Mesaros S, Brovkovych V, Kubaszewski E, Grunfeld S, et al. Mechanical transduction of nitric oxide synthesis in the beating heart. Circ Res 1997;81:372–9.
20. Mesaros S, Grunfeld S, Mesarosova A, Bustin D, Malinski T. Determination of nitric oxide saturated (stock) solution by chronoamperometry on a porphyrine microelectrode. Anal Chim Acta 1997;339:265–70.
21. Gyllenhammer H. Lucigenin chemiluminescence in the assessment of neutrophil superoxide production. J Immunol Methods 1987;97:209–13.
22. Ellis G, Adatia I, Yazdanpanah M, Makela SK. Nitrite and nitrate analyses: a clinical biochemistry perspective. Clin Biochem 1998; 31:195–220.
23. Wang P, Zweier JL. Measurement of nitric oxide and peroxynitrite generation in the postischemic heart. J Biol Chem 1996;271: 29223–30.
24. Cook S, Duplam H, Egli M, Scherrer U. Direct evidence for decreased vascular nitric oxide synthesis in mice with disruption of the gene for endothelial nitric oxide synthase [Abstract]. FASEB J 2000;14:A118.
25. Mackenzie IMJ, Ekangaki A, Young JD, Garrard CS. Effect of renal function on serum nitrogen oxide concentrations. Clin Chem 1996;42:440–4.
26. Mayer B, Andrew P. Nitric oxide synthase: catalytic function and progress toward selective inhibition. Naunyn Schmeidebergs Arch Pharmacol 1998;358:127–33.
27. Smith SD, Wheeler MA, Weiss RM. Nitric oxide synthase: an endogenous source of elevated nitrite in infected urine. Kidney Int 1994;45:586–91.
28. Wheeler MA, Smith SD, Garcia-Gardena G, Nathan CF, Weiss RM, Sessa WC. Bacterial infection induces nitric oxide synthase in human neutrophils. J Clin Invest 1997;99:110–6.
29. Nagase S, Takemura K, Ueda A, Hirayama A, Aoyagi K, Kondoh M, Koyama A. A novel nonenzymatic pathway for the generation of nitric oxide by the reaction of hydrogen peroxide and D- or L-arginine. Biochem Biophys Res Commun 1997;233:150–3.
30. Vetrovsky P, Stoclet JC, Entlicher G. Possible mechanism of nitric oxide production from N^G-hydroxy-L-arginine or hydroxylamine by superoxide ion. Int J Biochem Cell Biol 1996;28:1311–8.
31. Modolell M, Eichmann K, Soler G. Oxidation of *N*(G)-hydroxyl-L-arginine to nitric oxide mediated by respiratory burst: an alternative pathway to NO synthesis. FEBS Lett 1997;401:123–6.
32. Hollenberg SM. Inhibition of nitric oxide synthase in sepsis: a primary strategy? Crit Care Med 1998;26:638–9.
33. Lundberg JON, Carlsson S, Engstrand L, Morcos E, Wiklund NP, Weitzberg E. Urinary nitrite: more than a marker of infection. Urology 1997;50:189–91.
34. Lincoln J, Hoyle CHV, Burnstock G. Nitric oxide in health and disease. Cambridge: Cambridge University Press, 1997:103–36.
35. Kröncke K-D, Fehsel K, Kolb-Bachofen V. Inducible nitric oxide synthase in human disease. Clin Exp Immunol 1998;113:147–56.
36. Chen AFY, O'Brien T, Katusic ZS. Transfer and statement of recombinant nitric oxide synthase gene in the cardiovascular system. TIPS 1998;19:276–86.
37. Huk I, Nanobashvili J, Neumaayer C, Punz A, Mueller M, Afkhampour K, et al. L-Arginine treatment alters the kinetics of nitric oxide and superoxide release and reduces ischemia/reperfusion injury in skeletal muscle. Circulation 1997;96:667–75.
38. Klatt P, Schmidt K, Uray G, Mayer B. Multiple catalytic functions of brain nitric oxide synthase. J Biol Chem 1994;268:14781–7.